Electron dynamics in high energy density plasma bunch generation driven by intense picosecond laser pulse

Cite as: AIP Advances **8**, 055012 (2018); https://doi.org/10.1063/1.5023283
Submitted: 23 January 2018 • Accepted: 06 May 2018 • Published Online: 14 May 2018

M. Li, T. Yuan, Y. X. Xu, et al.

Electron dynamics in high energy density plasma bunch generation driven by intense picosecond laser pulse

M. Li,[1,a] T. Yuan,[2] Y. X. Xu,[3] and S. N. Luo[1,4]
[1]*The Peac Institute of Multiscale Sciences, Chengdu, Sichuan 610031, China*
[2]*Key Laboratory for Laser Plasmas (Ministry of Education) and School of Physics and Astronomy, Shanghai Jiao Tong University, Shanghai 200240, China*
[3]*State Key Laboratory of Precision Spectroscopy, East China Normal University, Shanghai 200062, China*
[4]*Key Laboratory of Advanced Technologies of Materials, Ministry of Education, Southwest Jiaotong University, Chengdu, Sichuan 610031, China*

(Received 23 January 2018; accepted 6 May 2018; published online 14 May 2018)

When an intense picosecond laser pulse is loaded upon a dense plasma, a high energy density plasma bunch, including electron bunch and ion bunch, can be generated in the target. We simulate this process through one-dimensional particle-in-cell simulation and find that the electron bunch generation is mainly due to a local high energy density electron sphere originated in the plasma skin layer. Once generated the sphere rapidly expands to compress the surrounding electrons and induce high density electron layer, coupled with that, hot electrons are efficiently triggered in the local sphere and traveling in the whole target. Under the compressions of light pressure, forward-running and backward-running hot electrons, a high energy density electron bunch generates. The bunch energy density is as high as TJ/m^3 order of magnitude in our conditions, which is significant in laser driven dynamic high pressure generation and may find applications in high energy density physics. https://doi.org/10.1063/1.5023283

How to produce extremely high pressure in laboratory is of critical importance in high pressure physics, which can find applications in material science,[1–3] high energy density physics,[4,5] laboratory astrophysics[6,7] and laser fusion[8–10] etc. In the past decades, the intense laser driven dynamic high pressure has attracted much attention due to its low cost, short experimental period and fine controllability.[11–14] When a solid target is irradiated by an intense laser pulse, a strongly heated and highly pressurized frontal layer will form through the energy absorption from the laser pulse (stage I) and then shock wave will produce and propagate in the undisturbed solid target (stage II). For their different characteristics, stage I is usually described by the hydrodynamics model[15,16] while stage II can be simulated by molecular dynamic method.[17] Recently, due to the fast development in the controlling of short intense laser pulses and the fabrication of nanometer targets, people are beginning to consider the laser loading with short duration laser pulses, e.g. ps or fs laser, upon submicrometer films. For this new situation, hydrodynamic model, which has superiority in describing the physical phenomena in the nanosecond time scale and micrometer length scale, meets great challenges since the single-particle dynamics becomes significant in the interactions. To appropriately describe the particle dynamics, the particle-in-cell (PIC) simulation is an effective and efficient way. Li et al. investigated the physics in stage I with PIC method and find that pressure as high as 0.13 TPa can be generated after the laser pulse with intensity 10^{15} W/cm^2 and 5 ps pulse duration is injected upon a nanometer solid density plasma.[18,19] The peak pressure is shown to be resulted from an high energy density plasma bunch produced through plasma implosion under extremely high light pressure. Although it is significant importance in the extremely dynamic high pressure generation, the

[a]Electronic mail: mli@pims.ac.cn

dynamics of high energy density plasma bunch is not so clear. Hence, in this letter, we amply simulate the process of high energy density plasma bunch generation and analyze its underlying physical mechanism. For the length limit, we just discuss the electron dynamics in the high energy density plasma bunch generation in this letter. All the calculations are carried out by the software package VORPAL[20] developed by Tech-X company.

Fig. 1 shows the schematic diagram of our physical model, in which an intense ps laser pulse with intensity 10^{16} W/cm^2 propagating along the positive direction of x axis normally irradiates a solid film described by a pre-formed plasma with a density near the plasma critical density, so called pre-plasma. The pre-plasma is comprised of singly-charged hydrogen ions and electrons with the mass ratio $m_i/m_e = 1836$, where m_i and m_e are the ion and electron masses, respectively. The plasma pressure is calculated by its microscopic definition,

$$p \equiv \frac{dI}{dtdA} = \sum_{i,v_{ix}>0} n_i m v_{ix}^2, \tag{1}$$

where dI is the total particle momentum impinging upon an area dA in a period of time dt, n_i is the number density of particles with velocity v_i, v_{ix} is the x component of velocity, and m is the particle mass. In relativistic conditions, Eq. (1) can be rewritten as,

$$\begin{aligned} p &= \sum_{i,v_{ix}>0} n_i \gamma_i m_0 v_{ix}^2 \\ &= m_0 c^2 \sum_{i,v_{ix}>0} n_i \frac{u_{ix}^2}{\gamma_i c^2} \\ &= m_0 c^2 n|_{u_x>0} \left\langle \frac{u_x^2}{\gamma c^2} \right\rangle. \end{aligned} \tag{2}$$

Where m_0 is the rest mass of particle, c is light speed in vacuum, $n|_{u_x>0}$ is the number density of particles running in the positive x direction and $\langle \cdots \rangle$ denotes the corresponding average. $\gamma = 1/\sqrt{1 - v^2/c^2}$ is the Lorentz factor and $u_x = \gamma v_x$. If one considers the particles with $u_x < 0$, the calculated pressure is acting on the negative x direction.

Through intensive calculations, some optimal laser and plasma parameters that prompt to produce extremely high pressure are found in former works.[18,19] Here we substantially adopt those optimal parameters but change few of them just to increase the computational efficiency. New parameter assemble is as follows: a linear polarized plane wave pulse with wavelength $\lambda = 0.4\mu$m, intensity $I = 10^{16}$ W/cm^2 and pulse duration $\tau = 1$ ps is injected upon a pre-plasma target with initial density $n_0 = 2n_c = 1.393 \times 10^{28}$ m^{-3}, thickness $d = 0.2\lambda$ and initial temperature $T_0 = 1000$ K, where $n_c = \pi m_e c^2/e^2\lambda^2$ is plasma critical density, m_e and e are electron mass and electron charge, respectively. The physical model can produce an extremely high pressure with its peak value up to TPa order of magnitude in the target, which is mainly due to a high energy density plasma bunch generated in the target (see Fig. 2).

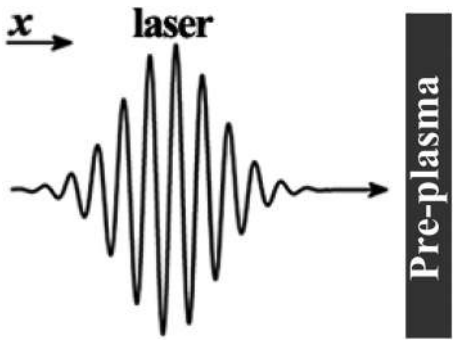

FIG. 1. Schematic diagram of the physical model. The laser wavelength is $\lambda = 0.4\mu$m and the pulse duration is $\tau = 1$ ps. The thickness of the pre-plasma target is $d = 80$ nm.

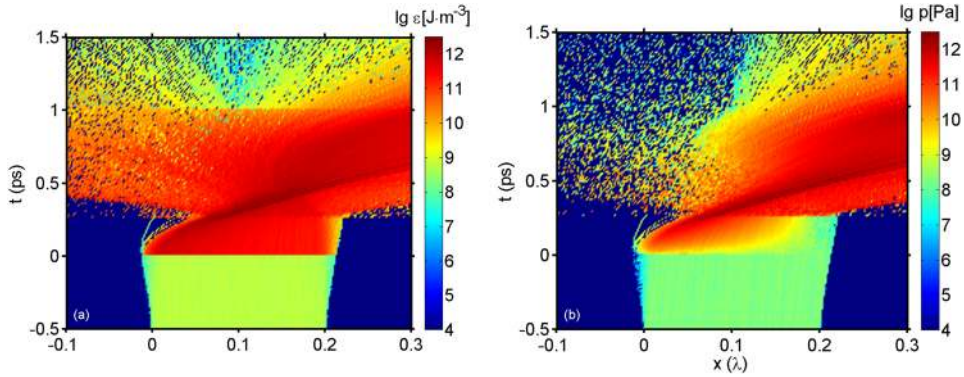

FIG. 2. Spatial and temporal evolution of (a) plasma energy density and (b) plasma pressure. Physical quantities are plotted in their logarithmic forms. The laser pulse starts to interact with the target at $t = 0$ ps and the pre-plasma target sits in $x = 0 \sim 0.2\lambda$.

To investigate how this bunch is generated, we firstly plot the number density and pressure of forward-running and backward-running electrons, respectively in Fig. 3. As is shown in Fig. 3, the laser pulse continuously driven electric currents and return currents in the target especially in the plasma skin layer ($\sim$ 10 nm) until $t \sim 250$ fs when hot electrons generated due to enough energy density ($\sim$ TJ/m^3) of the skin layer. Once generated the hot electrons transport in the whole target with a velocity $v_{hef} \sim 9.67 \times 10^6$ m/s. At the spatial and temporal key point R, the hot electrons arrived at the target rear surface for the first time and some of them rushed out resulting in an intense sheath field which inversely forces electrons to comeback. The coming back hot electrons immediately form hot electric return current transporting in the target with a velocity $v_{heb} \sim 8.96 \times 10^6$ m/s. At the spatial and temporal key point S, the hot electric return current arrived at the right side of the skin layer, which results in the obvious increase of the density in the right side of the skin layer due to the intense compression induced by the returning hot electrons. With the time evolution, more and more hot electric currents and their return currents are induced. The forward compressions of light

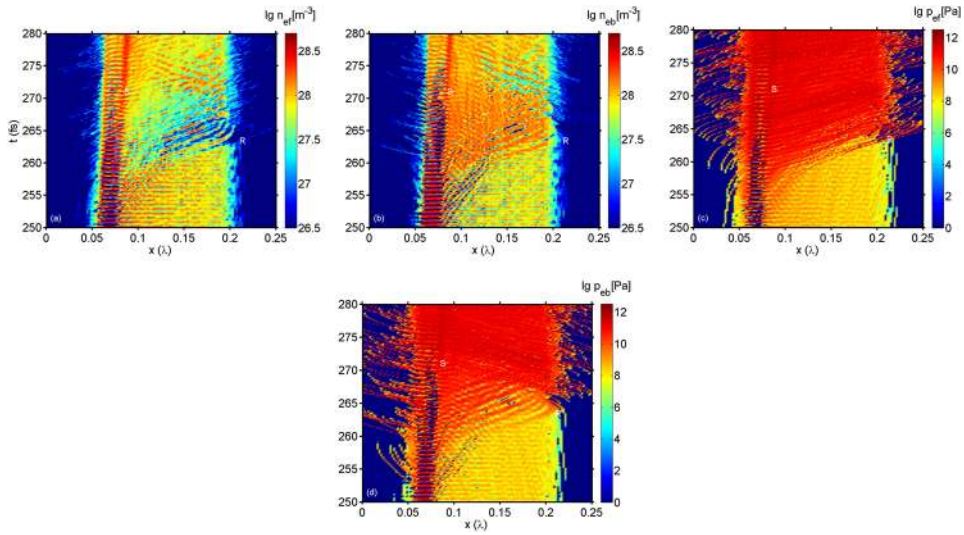

FIG. 3. Spatial and temporal evolution of (a) number density of forward-running electrons, (b) number density of backward-running electrons, (c) pressure of forward-running electrons, and (d) pressure of backward-running electrons, respectively. Two spatial and temporal key points R and S are marked in the figure with their coordinates R(0.21,263.4), and S(0.085,271.5) in space and time, respectively. Physical quantities are plotted in their logarithmic forms. The simulation parameters are as same as Fig. 2.

pressure (~ 333.52 GPa) and forward-running hot electrons together with the backward compression of the returning hot electrons finally induce the high energy density electron bunch (HEDEB).

For the important role played by the hot electrons in the generation of HEDEB, we divide all electrons into cold subsystem and hot subsystem according to their kinetic energy E_k, namely, electrons with kinetic energy under a critical value E_{kc} are cold while the other are hot, where E_{kc} is defined as $E_{kc} = 0.5E_{km}$ and E_{km} is the maximum kinetic energy a free electron can obtain in the laser field, respectively. In our condition $E_{km} \sim 298.3935$ eV. After this classification we plot the spatial and temporal evolution of the cold subsystem and hot subsystem of corresponding electron density in Fig. 4. As assistant analysis, the x component of electric field E_x and the unclassified electron density are also plotted in the figure.

As is shown in Fig. 4, when classified according to kinetic energy, the spatial and temporal evolution of electron density demonstrates a drivage model in the target frontal layer with a thickness $d_{fl} \sim 20$ nm (Fig. 4(c) and (d)), which can affect the generation of HEDEB. As is not the main topic in this letter, the mechanism underlying the drivage model is not discussed. Qualitatively speaking, it is dominated by the checks and balances of electron energy density, electron pressure, electromagnetic field energy density and light pressure in the drivage surface. The evolution of the drivage surface in the spatial and temporal evolution figure of electron density is called drivage wave. Generally, a drivage wave starts with considerable hot electrons coming back from the left vacuum (see point C in Fig. 4) and comes to an end with considerable hot electrons rushing out (see point F in Fig. 4).

From the spatial and temporal evolution of hot electron density shown in Fig. 4(d), we can see that a localized dense sphere of hot electrons with energy density up to TJ/m^3 order of magnitude forms at $x \sim 0.067\lambda$ and $t \sim 253$ fs. For high energy density, the sphere expands rapidly in both directions of x axis, which results in the density increase on its left and right sides. When the time evolves to $t \sim 261$ fs, numerous hot electrons that can penetrate the whole target are trigged (marked as point B in Fig. 4(d)). The forward-running hot electrons transit through the target and forms the return hot electrons under the force of the sheath field near the target rear surface while the backward-running hot electrons partially breaks the dense folium and rushed out of the front surface, which leads to the intensive loss of hot electrons (Fig. 4(d)) and thus induces intense positive electric field in the

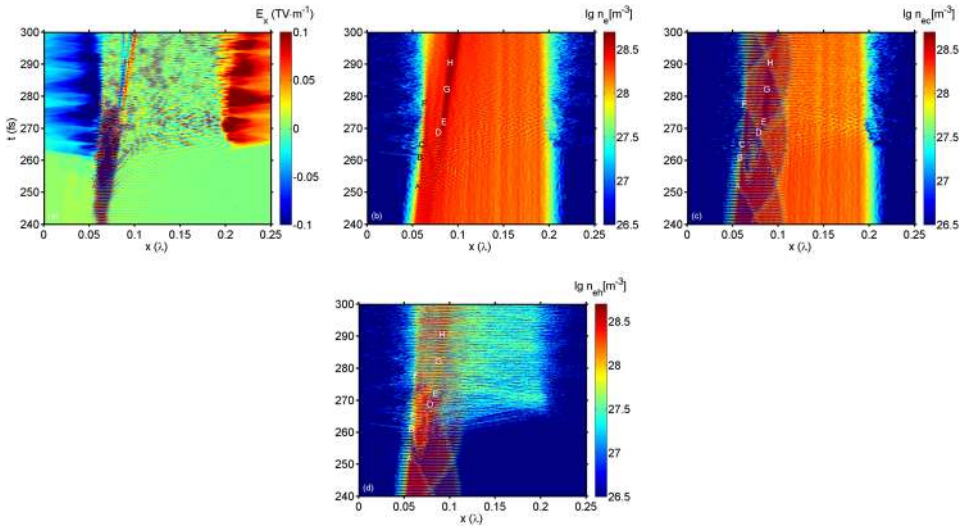

FIG. 4. Spatial and temporal evolution of (a) x component of electric field, (b) number density of unclassified electrons, (c) number density of cold electrons, and (d) number density of hot electrons, respectively. Cold electrons are those whose kinetic energy is less than a critical value E_{kc} defined as $E_{kc} = 0.5E_{km}$, while those with $E_k > E_{kc}$ are hot ones, where $E_{km} \sim 298.3935$ eV is the maximum kinetic energy a free electron can be accelerated by the laser field. Some spatial and temporal key points are marked in the figure, whose coordinates in space and time are A(0.053,252), B(0.055,261), C(0.057,265), D(0.075,268.7), E(0.0815,271.5), F(0.06,277.56), G(0.084,282.15), and H(0.088,290.35), respectively. Physical quantities are plotted in their logarithmic forms. The simulation parameters are as same as Fig. 2.

target region between point B and C (Fig. 4(a)). The rushing out hot electrons in the target front surface produce a kick upon the cold electrons and the coming back hot electrons from vacuum also compress the cold electrons, which makes the density of cold electrons increase near the target front surface (Fig. 4(c)). Point C in Fig. 4 indicates the start of a drivage wave related to intense returning hot electron current from vacuum, which cracks the dense cold electron folium into two parts. One part named as pre-electron-bunch (PEB) transports along the drivage wave (C-D in Fig. 4(c)), the other keeps in the target front surface (C-F in Fig. 4(c)). At point D the drivage wave is collided by another one, which slightly changes the evolution path of PEB (Fig. 4(c)). Then the PEB meets the pre-compressed dense electron folium on the right side of the hot electron sphere (Fig. 4(b) and (d)), which violently changes the evolution path of PEB and increases its density. Soon, the returning hot electrons from the target rear surface arrive at the PEB (point E in Fig. 4(d)) resulting in an energetic compression onto the PEB. The intense compressions of light pressure, forward-running and backward-running hot electrons make the PEB density remarkably increase and finally trigger the formation of the HEDEB (E-G in Fig. 4(b)).

It is clear that the drivage wave can affect the generation of HEDEB. Actually it also affects its transportation in the target. As is collided by the drivage wave, a few electrons in HEDEB may be decelerated and separate from the parent substance even form a new electron bunch whose transport velocity is lower than the original one (point H in Fig. 4(b)). This is a crucial reason why the HEDEB splits and desaturates in its evolution path. In applications of high energy density particle bunch, a low energy spread, small divergence angle and high density bunch is needed. So we need to weaken the influence of the drivage wave in these applications. It is worth to note that the high energy density plasma bunch generation can be found tremendous similarity to the plasma block generation based on the skin layer acceleration by nonlinear forces,[10,21,22] which is confirmed in theoretical[21,23,24] and experimental[25–28] researches and has already been used in the fusion ignition, e.g. PW-ps laser induced plasma block-ignition in fusion reaction of protons with the isotope of boron.[8–10] The ultrahigh particle density of the plasma block is million times higher than that obtained in all classical accelerators, which can induce extremely high pressure and easily satisfy the ignition requirements of the proton-boron fusion reaction. The forward-running plasma bunch shown in this work is similar to the plasma blocks induced through the skin layer acceleration by nonlinear forces,[10,21] which proves that the high energy density plasma bunch is significant in laser driven dynamic high pressure physics and may find potential applications in high energy density physics.

In summary, through one dimensional PIC method, we investigated the electron dynamics of the high energy density plasma bunch generation with an intense picosecond laser pulse loaded upon a sub-micrometer dense plasma target. The HEDEB generation is mainly due to a laser driven dense and hot electron sphere which rapidly expands and triggers numerous hot electrons traveling in the whole target. Under the compressions of light pressure, forward-running and backward-running hot electrons, the HEDEB efficiently generate. It should be reminded that we just revealed how the HEDEB is induced in this work. Actually the ions also play an important role. Moreover, a thick solid target is usually attached to the rear surface of the pre-plasma target, which will absorb the energy imparted from the pre-plasma and induce an intense shock pressure in the solid target. These issues are all attractive, which will be considered in future work including laser boron fusion.[29]

We thank Y. Yu in Shanghai Institute of Optics and Fine Mechanics, Chinese Academy of Sciences for fruitful discussion. The computations were performed at the Supercomputing Center of the Peac Institute of Multiscale Sciences. This work is supported by the Science Challenge Project of China (No. TZ2018001), and the National Natural Science Foundation of China (No. 11627901).

[1] M. A. Meyers, F. Gregori, B. K. Kad, M. S. Schneider, D. H. Kalantar, B. Remington, G. Ravichandran, T. Boehly, and J. S. Wark, Acta Mater. **51**, 1211 (2003).
[2] B. A. Remington, G. Bazan, and J. Belak, Metall. Mater. Trans. A **35**, 2587 (2004).
[3] B. A. Remington, P. Allen, E. M. Bringa, J. Hawreliak, D. Ho, K. T. Lorenz, H. Lorenzana, J. M. Mcnaney, M. A. Meyers, and S. W. Pollaine, Mater. Sci. Tech. **22**, 474 (2006).
[4] R. P. Drake, L. Davison, and Y. Horie, *High-Energy-Density Physics* (Springer Berlin Heidelberg, 2006).
[5] R. P. Drake, Phys. Plasmas **16**, 627 (2009).
[6] Y. Kuramitsu, H. H. Chu, L. N. Hau, S. H. Chen, Y. L. Liu, C. Y. Hsieh, Y. Sakawa, T. Hideaki, J. Wang, and Y. Kuramitsu, High Energ. Dens. Phys. **17**, 198 (2015).

[7] S. V. Bulanov, T. Z. Esirkepov, M. Kando, J. Koga, K. Kondo, and G. Korn, Plasma Phys. Rep. **41**, 1 (2015).
[8] C. Labaune, C. Baccou, S. Depierreux, C. Goyon, G. Loisel, V. Yahia, and J. Rafelski, Nat. Commun. **4**, 2506 (2013).
[9] A. Picciotto, D. Margarone, A. Velyhan, P. Bellutti, J. Krasa, A. Szydlowsky, G. Bertuccio, Y. Shi, A. Mangione, and J. Prokupek, Phys. Rev. X **4**, 031030 (2014).
[10] H. Hora, G. Korn, L. Giuffrida, D. Margarone, A. Picciotto, J. Krasa, K. Jungwirth, J. Ullschmied, P. Lalousis, and S. Eliezer, Laser Part. Beam. **33**, 607 (2015).
[11] L. B. D. Silva, P. Celliers, G. W. Collins, K. S. Budil, N. C. Holmes, T. W. Barbee, B. A. Hammel, J. D. Kilkenny, R. J. Wallace, and M. Ross, Phys. Rev. Lett. **78**, 483 (1997).
[12] D. Batani, A. Balducci, D. Beretta, A. Bernardinello, T. Löwer, M. Koenig, A. Benuzzi, B. Faral, and T. Hall, Phys. Rev. B **61**, 9287 (2000).
[13] D. Batani, H. Stabile, A. Ravasio, T. Desai, G. Lucchini, F. Strati, J. Ullschmied, E. Krousky, J. Skala, and B. Kralikova, Laser Part. Beam. **21**, 481 (2003).
[14] D. C. Swift, R. A. Kopp, and J. T. Gammel, Phys. Rev. E **69**, 036406 (2004).
[15] K. Eidmann, J. Meyer-ter Vehn, T. Schlegel, and S. Hüller, Phys. Rev. E **62**, 1202 (2000).
[16] V. K. Senecha, J. Zhang, W. Wang, and H. C. Pant, Acta Phys. Sinica **50**, 10917 (2001).
[17] Z. Gu, C. Sun, J. Zhao, and N. Zhang, J. Appl. Phys. **96**, 3486 (2004).
[18] M. Li, J. X. Wang, Y. X. Xu, and W. J. Zhu, Phys. Plasmas **24**, 013117 (2017).
[19] M. Li, J. X. Wang, T. Yuan, Y. X. Xu, and W. J. Zhu, AIP Adv. **7**, 035007 (2017).
[20] C. Nieter and J. R. Cary, J. Comput. Phys. **196**, 448 (2004).
[21] H. Hora, Czech. J. Phys. **53**, 199 (2003).
[22] H. Hora, J. Badziak, M. N. Read, Y. T. Li, T. J. Liang, C. Yu, H. Liu, Z. M. Sheng, J. Zhang, and F. Osman, Phys. Plasmas **14**, 072701 (2007).
[23] H. Hora, Phys. Fluids **28**, 3705 (1985).
[24] H. Hora, *Laser Plasma Physics: Forces and the Nonlinearity Principle* (SPIE Press, Bellingham, WA, 2016).
[25] R. Sauerbrey, Phys. Plasmas **3**, 4712 (1996).
[26] A. A. Kozlov, J. Makowski, P. Parys, L. Ryc, J. Wolowski, E. Woryna, and A. B. Vankov, Laser Part. Beam. **17**, 323 (1999).
[27] J. Badziak, S. Glowacz, S. Jablonski, P. Parys, J. Wolowski, and H. Hora, Appl. Phys. Lett. **85**, 3041 (2004).
[28] J. Badziak, S. Glowacz, S. Jablonski, P. Parys, J. Wolowski, H. Hora, J. Krasa, L. Laska, and K. Rohlena, Plasma Phys. Contr. F. **46**, B541 (2004).
[29] H. Hora, S. Eliezer, G. J. Kirchhoff, N. Nissim, J. X. Wang, P. Lalousis, Y. X. Xu, G. H. Miley, J. M. Martinez-Val, W. Mckenzie, and J. Kirchhoff, Laser Part. Beams **35**, 730 (2017).